High-Temperature Superconductors: A Structural–Electronic Model

JEREMY K. BURDETT

Department of Chemistry, James Franck Institute and NSF Center For Superconductivity, The University of Chicago, Chicago, Illinois 60637

Received November 9, 1994

Introduction

An enormous amount of effort has been expended[1] in recent years in attempts to understand the fascinating properties of that class of complex copper oxides which are high-temperature superconductors. This activity has led to the generation of an unprecedented level of chemical and structural detail concerning this rather small region of the periodic table, renewed interest in the physics behind metal–insulator transitions in general, and a renaissance in the area of superconductivity itself. (For several years investigations had labored under the prediction that 30 K was probably the highest T_c attainable.) In spite of this activity, identification of the essential piece of the physics is lacking. This is puzzling since the magnitude of the effect, the high T_c's, should make this a rather straightforward phenomenon to explain.[2]

This Account will briefly summarize some of the salient features of the structural–electronic problem in the cuprates and will present a view of the electronic structure of these materials which may well be the chemical piece needed to complete the physical jigsaw puzzle.

Structural–Compositional Control of Superconductivity

The very large number of new superconducting copper oxides which have been characterized[3] are all derived structurally from the perovskite structure. It is possible, seven years after the work of Bednorz and Müller,[4] to make some generalizations concerning the chemical, structural, and compositional characteristics necessary for "high-temperature" (30–150 K) superconductivity.[5]

(i) Sheets of stoichiometry CuO_2 containing square-planar copper. These are frequently not flat and in addition often have extra oxygen atoms coordinated to copper but at much longer distances (2.3–2.8 Å) than those in the plane (~1.9–2.0 Å). All of the other atoms in the structure are assigned to a "reservoir" region[6] whose main function is to ensure an optimal copper oxidation state (see item ii). Most of the highest T_c's are associated with structures which have particularly flat sheets with very long Cu–O distances perpendicular to them, or no such oxygen at all.

(ii) A "magic" [5] copper oxidation state of around 2.15 for systems which do not contain mercury. In many systems (as in $La_{1.85}Sr_{0.15}CuO_4$ or $Tl_{1.17}Ca_{0.83}Ba_2Cu_2O_{6.75}$) this is easy to identify, but more frequently it is not possible to assign the copper oxidation state without a detailed structural and stoichiometric study. Such studies are often extremely difficult because of disorder, partial site occupancy, and incommensurate structures. Doping may also occur by band overlap (as in $YBa_2Cu_2O_7$)[6] or both overlap and nonstoichiometry. Here, knowledge of the formula is insufficient to identify the oxidation state. The critical oxidation state in some of the mercury-containing systems appears to be higher.[7]

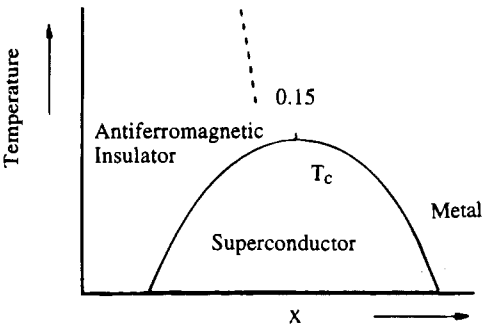

Figure 1. Schematic behavior of the transport properties of $La_{2-x}Sr_xCuO_4$ with x.

In a few systems,[1] such as $La_{2-x}Sr_xCuO_4$, the electronic picture may be studied experimentally as a broad function of doping level, x. The results are particularly interesting (Figure 1). For $x = 0$ the system is an antiferromagnetic insulator; a superconductor is generated as x increases, reaching a maximum T_c at around $x = 0.15$, the magic electron count; and with higher x (the "overdoped" region) superconductivity disappears and a normal metal results. Across the whole range the dimensions of the structure change smoothly.

(iii) "Correct" Cu–O distance. Even if the doping level is correct, a superconductor frequently does not

Jeremy Burdett was born in London, England, and was educated at the Universities of Cambridge and Michigan. He is currently professor in the Chemistry Department, The James Franck Institute and The College, at The University of Chicago. His research interests lie in the area of physical inorganic chemistry and include electronic and structural aspects of molecules and solids and their photochemistry and reactivity.

(1) A very useful source book: *Chemistry of High-Temperature Superconductors*; Vanderah, T. A., Ed.; Noyes: Park Ridge, NJ, 1991.
(2) Emery, V. J.; Kivelson, S. A. *Physica C* **1993**, *209*, 597.
(3) For some reviews, see: (a) *Chemistry of High-Temperature Superconductors*; ACS Symposium Series 351; American Chemical Society: Washington, DC, 1987; Nelson, D. L., Whittingham, M. S., George, T. F., Eds.; Nelson, D. L., George, T. F., Eds.; ACS Symposium Series 377; American Chemical Society: Washington, DC, 1988. (b) Sleight, A. W. *Science* **1988**, *242*, 1519, (c) Cava, R. J. *Science* **1990**, *247*, 656.
(4) Bednorz, J. G.; Müller, K. A. *Z. Phys. B. Con. Matter.* **1986**, *64*, 189.
(5) Burdett, J. K. *Inorg. Chem.* **1993**, *32*, 3915.
(6) Burdett, J. K. *Adv. Chem. Phys.* **1992**, *83*, 207.
(7) Radaelli, P. G.; Wagner, J. L.; Hunter, B. A.; Beno, M. A.; Knapp, G. S.; Jorgensen, J. D.; Hinks, D. G. *Physica* **1993**, *C 216*, 29.

0001-4842/95/0128-0227$09.00/0

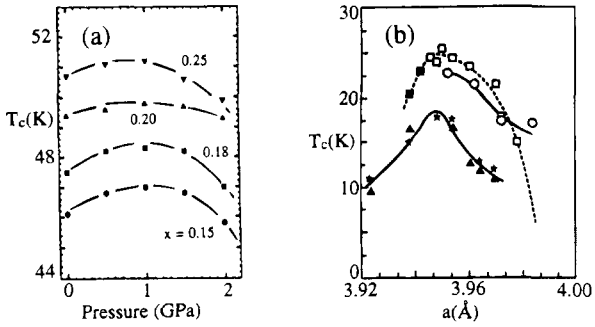

Figure 2. (a) Pressure dependence of T_c for $La_{2-x}Ca_{1+x}Cu_2O_6$ (adapted from ref 10). (b) Dependence of T_c on the size of the reservoir ions in $M_{1.85-x}M'_xM''_{0.15}CuO_4$ (adapted from ref 9): (□) M = Nd, M′ = La, M″ = Ce; (▲, ★) M = Eu, M′ = La, M″ = Ce; (○) M = Nd, M′ = La, M″ = Th; (■) M = Nd, M′ = Y, M″ = Ce. The abscissa is the a lattice parameter.

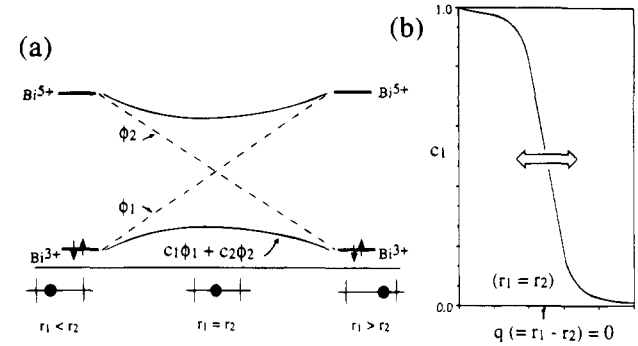

Figure 3. The electronic state of affairs in $Ba_{1-x}K_xBiO_3$. (a) Intersection of the Bi^{3+} and Bi^{5+} states to give the mixed valence system. At $r_1 = r_2$ ($q = 0$), $c_1 = c_2$. (b) Variation in c_1 with $r_1 - r_2$ ($q \neq 0$).

result. For example, the perovskite[8] $La_{1.85}Sr_{0.15}SnCuO_6$, which may be written as $(La_{1.85}Sr_{0.15}O_2)(SnO_2)(CuO_2)$ to highlight the reservoir and CuO_2 regions, has the correct copper oxidation state for superconductivity, but the Cu–O distance is far too large (~2 Å). The equilibrium Cu–O distance is influenced by two effects.[9] Since the energy levels involved in doping are copper–oxygen antibonding, there is the "electronic" effect controlled by the doping level. Increasing the number of holes thus shortens the Cu–O distance. There are steric demands of the reservoir region too as in this tin-containing example. Thus T_c may be varied (Figure 2) as a function of pressure[10] and by the systematic variation of the size of the cations in the reservoir region.[9] An important feature of these plots is the very small change in interatomic separation involved. The half-width of the peaks of Figure 2b is about 0.06 Å. Using the observed[1] pressure dependence of Cu–O distances, we find a similar figure for this parameter from the data of Figure of 2a. Thus the superconductivity phenomenon in these oxides takes place over a very short range of configuration (r(Cu–O)) space. This is not true for the Whangbo–Torardi plots of ref 11 since here the bond lengths are changing with doping level too.

Although a "magic" electronic configuration and special geometry at copper appear to be important conditions for the observation of superconductivity in these cuprates, there is another observation which a theory needs to be able to explain. Generation of the optimal superconducting composition is associated with a thermodynamic stabilization. Experimentally the system is often guided toward the superconducting composition, either during the initial synthesis step or later. In a study[12] of the series of oxides $Pb_2Sr_2RECu_3O_8$, where RE = rare earth, it was found that those examples with the larger REs (e.g., La) are semiconductors, but those with the smaller REs are superconductors with T_c's as high as 70 K. X-ray diffraction studies show that the superconducting samples with, e.g., RE = Ho, contain around 9% vacancies on the RE site, whereas this site is fully occupied in the insulating examples. Using this figure of 9% RE vacancies for the superconductors, and noting that $^2/_3$ of the copper atoms lie in the sheets (the third copper atom is present as Cu(I) in the reservoir region), a value of 2.14 is found for the in-sheet copper oxidation state. Thus there is some feature of the chemistry which, during the synthetic step, drives the system to chemically attain the magic electron count.

Samples of oxygen-rich $La_2CuO_{4+\delta}$ undergo[13] a phase separation at around room temperature of the form $La_2CuO_{4+\delta} \rightarrow La_2CuO_4 + La_2CuO_{4.07}$. $La_2CuO_{4.07}$ is a superconductor, and the copper oxidation state is 2.14 here too. In a study on the Tl/Ca/Ba/Cu/O system[14] the $Tl_{1.17}Ca_{0.83}Ba_2Cu_2O_{6.75}$ phase (the superconductor with the magic doping level) emerges as the most stable under the synthesis conditions. Here are two more examples of this unusual stabilization effect.

Intersection of Electronic States and Superconductivity in Ba/K/Bi/O

One mechanism for superconductivity involves the generation of an attractive potential between a pair of electrons (Cooper pair) induced by strong electron–phonon coupling. The BCS model has been very useful for understanding many facets of this mechanism. To begin to tie together parts of the chemistry and physics, we will use here not a cuprate but a closely related system, that of $Ba_{1-x}K_xBiO_3$. $BaBiO_3$ is an insulator which on doping with potassium gives a 30 K superconductor. The structure[1] of the undoped material is that of a distorted perovskite containing "small" and "large" octahedra indicating a Bi^{4+} which has disproportionated into Bi^{3+} and Bi^{5+} with different geometries at each site. When the system is doped with potassium, this arrangement is suppressed and the Bi–O distances become equal. We can describe the electronic state of affairs in a useful way as the result of the intersection of two electronic states as a function of the local Bi–O bond length asymmetry (Figure 3a). (A very similar description is used for inner-sphere electron transfer reactions of transition

(8) Anderson, M. T.; Poeppelmeier, K.; Gramsch, S. A.; Burdett, J. K. *J. Solid State Chem.* **1993**, *102*, 164.
(9) Wang, E.; Tarrascon, J.-M.; Greene, L. H.; Hull, G. W.; McKinnon,W. R. *Phys. Rev.* **1990**, *B41*, 6582.
(10) Yamada, Y.; Kinoshita, K.; Matsumoto, T.; Izumi, F.; Yamada, T. *Physica* **1991**, *C185–189*, 1299.
(11) Whangbo, M.-H.; Torardi, C. C. *Science* **1990**, *249*, 1143; *Acc. Chem. Res.* **1991**, *24*, 127.
(12) Xue, J. S.; Reedyk, M.; Greedan J. E.; Timusk, T. *J. Solid State Chem.* **1993**, *102*, 492. Xue, J. S.; Greedan J. E.; Maric, M. *Ibid.* 501.
(13) Jorgensen, J. D.; Dabrowski, B.; Pei, S.; Hinks, D. G.; Soderholm, L.; Morosin, B.; Schirber, J. E.; Venturini, E. L.; Ginley, D. S. *Phys. Rev.* **1988**, *B38*, 11337. Jorgensen, J. D.; Dabrowski, B.; Richards, D. R.; Hinks, D. G. *Phys. Rev.* **1989**, *B40*, 2187.
(14) E.g.: Kaneko, T.; Yamaguch, H.; Tanaka, S. *Physica* **1991**, *C 178*, 377.

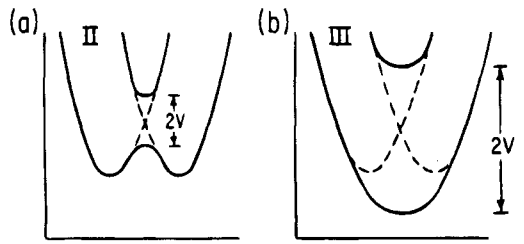

Figure 4. Conventional description of mixed valence compounds of type I or II (a) and of type III (b). The abscissa is some geometrical coordinate.

metal complexes.) The interaction between the two states is nonzero, and for $r_1 = r_2$ (the point at which q, the displacement from the crossing point of the two dashed curves, equals 0) the ground state is described by equal contributions from Bi^{3+} and Bi^{5+} on both bismuth atoms ($c_1 = c_2$). The behavior of (say) c_1 as the O atom is moved from left to right is given by Figure 4b. On vibration around the point for which $q = 0$ ($c_1 = c_2$), shown by a double-headed arrow, the wave function thus changes to one where there is now an asymmetry ($c_1 \neq c_2$) when $q \neq 0$. One of the bismuth atoms is more "Bi^{3+}-like" and the other more "Bi^{5+}-like". Thus there is coupling between electronic and vibrational degrees of freedom. The variation in wave function is roughly linear over the region of vibration (Figure 3b), and thus the electron–phonon interaction remains constant.

Electronically the $Ba_{1-x}K_xBiO_3$ problem is interesting. The parent compound is a class I or class II compound in the Robin–Day sense,[15] but the doped system is certainly a class III system. The parent is an insulator, the doped compound a metal. Figure 4 shows how the relationship between the two is commonly described and involves the interaction between the "Bi^{3+}" and "Bi^{5+}" curves which leads to a stabilization of the mixed valence system in a variant of the picture of Figure 3a. The two curves correspond to two adjacent bismuth atoms with different oxidation states.

Superconductivity in materials of this type is tackled by BCS theory.[16] A constant electron–phonon interaction V is assumed to exist around the Fermi level over a range of $\pm h\omega_D$. $N(e_f)$ is the electronic density of states at the Fermi level, and in the limit of small $\lambda = N(e_f).V$ (weak coupling), $kT_c = 1.13h\omega_D \exp(-1/\lambda)$. There is an isotope effect associated with T_c since ω_D, a vibrational frequency, depends on the atomic masses involved. Obviously the larger λ, the higher T_c.

One route to put some chemistry into this formalism is via evaluation of the parameter Δc_1^2, the change in the character of the wave function over the amplitude of vibration. Because of the linear dependence of c_1 on distance over the region of interest, $\Delta c_1^2 \approx (\Delta r)^2$. Since for a harmonic oscillator $(1/2)k(\Delta r)^2 \approx h\nu \approx h(k/\mu)^{1/2}$, $\Delta c_1^2 \approx (1/\mu)^{1/2}$. Thus the functional dependence of T_c on mass from the BCS theory is identical to that using Δc_1^2 as a measure. $T_c/T_c' = (\Delta c_1^2)/(\Delta c_1^2)' = (\mu'/\mu)^{1/2}$. The connection between this electronic picture and the physics of the problem may be strengthened. By going beyond BCS theory it has been shown[17] from Eliashberg theory that it is probably not λ which determines high T_c values in strong-coupled superconductors but the area A under the electron–phonon spectral function and its shape. Under certain conditions T_c grows linearly with A. This is directly connected with the parameter Δc_1^2, which measures how much of the available coupling may be captured during the amplitude of a vibration. This concept will be useful later.

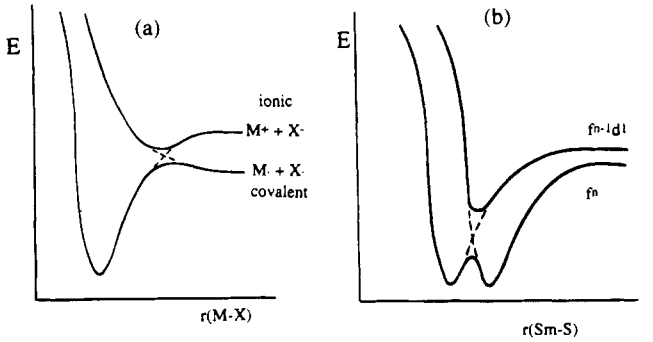

Figure 5. (a) Avoided crossing of ionic and covalent curves for NaCl. (b) Behavior of localized (insulator) and delocalized (metallic) states with metal–nonmetal distance in SmS, for example. The interaction between the two curves at their crossing ($q = 0$) is weak.

Metal Insulator Transitions: SmS and the Cuprates

The intersection of two diabatic states as in Figure 4 as a function of geometry occurs in many parts of chemistry. Perhaps the most famous[18] is that for the ionic and covalent curves of NaCl (Figure 5a). Here the intersection occurs in a region away from the equilibrium geometry of the system. Figure 5b shows a picture relevant to metal–insulator transitions, applicable to SmS, for example.[19] Two curves are shown, one corresponding to an insulator (f^n) and the other to a metal ($f^{n-1}d^1$), which lie close in energy. By squeezing of SmS an insulator-to-metal transition may be induced. There is a weak interaction between the two diabatic curves. A single parameter, η, is sufficient to characterize their behavior when their energy varies linearly with some configurational coordinate, q. ($q = 0$ corresponds to the crossing point of the diabatic curves just as in Figures 3 and 5.) η is just the ratio of their relative slopes to the interaction (H_{12}) between them. Figure 6 shows in general how the wave function changes and how the effective coupling (I) between the two curves varies as a function of η.

A related picture is applicable to doping-induced insulator–metal transitions in materials such as $La_{1-x}Sr_xMnO_3$ and $La_{1-x}Sr_xCuO_4$. In general terms the energy of atomic levels changes as a function of charge, and thus the relative energies of the two curves may be adjusted by varying the metal oxidation state. Figure 7 shows how the relative energies of the diabatic and adiabatic states vary with doping. Panel a corresponds to the undoped case, the insulator, and panel b to the doped metallic case. An insulator-to-

(15) Robin, M. B.; Day, P. *Adv. Inorg. Chem. and Radiochem.* **1967**, *10*, 247.
(16) Schrieffer, J. A. *Theory of Superconductivity*; Benjamin: Reading, MA, 1964.
(17) Leavens, C. R.; Cabotte, J. P. *J. Low Temperature Phys.* **1974**, *14*, 195.
(18) Mulliken, R. S. *J. Chim. Phys. Phys.-Chim. Biol.* **1964**, *61*, 20.
(19) Varma, C. M. *Rev. Mod. Phys.* **1976**, *48*, 218. Wilson, J. A. *Struct. Bonding* **1977**, *32*, 58.
(20) Burdett, J. K. *J. Solid State Chem.* **1992**, *100*, 393.

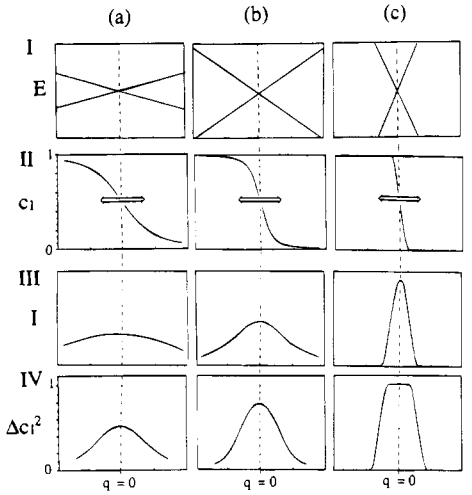

Figure 6. Some of the properties of importance for curve crossings. Columns a, b, and c represent increasing values of η, the ratio of the relative slopes of the two linear diabatic curves (ϕ_1,ϕ_2) to the interaction (H_{12}) between them. The coordinate q measures displacement from the crossing point. Row I shows three cases which essentially vary only in the relative slopes of ϕ_1 and ϕ_2. Row II shows the variation in wave function (c_1) with q. The wave function describing the lower adiabatic state is written as $c_1\phi_1 + c_2\phi_2$. Row III shows how the effective interaction (I) of the two diabatic states varies with q. The maximum of course is at $q = 0$. Row IV shows the variation in Δc_1^2 for a given amplitude of vibration. A fixed amplitude of vibration at $q = 0$ is shown in row II.

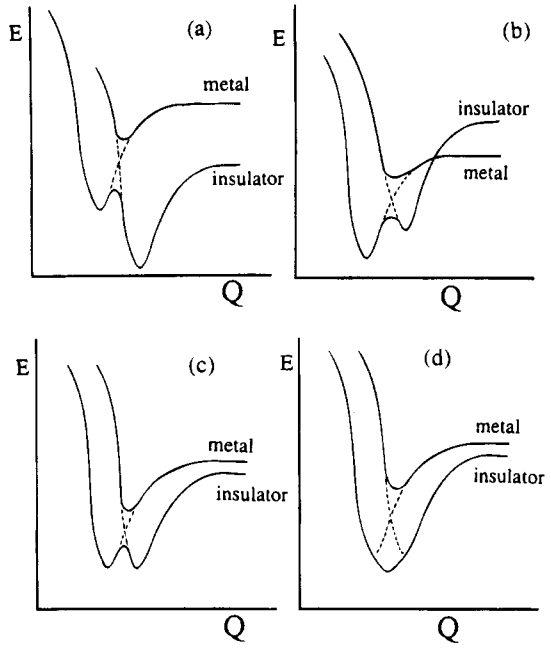

Figure 7. Variation in the relative energies of insulating and metallic states with doping: (a) an insulator, (b) a metal, (c) the point of a metal–insulator transition in $La_{1-x}Sr_xMnO_3$, for example, and (d) interaction between the two curves leading to a single minimum as in $La_{1-x}Sr_xCuO_4$ and the cuprates when the curves are close together in energy and Q-space. The curves are shown in panels c and d displaced from each other for clarity, but the maximum interaction in panel d will occur when the two minima have the same value of Q (=r(Cu–O) in the cuprates). Q is some configurational coordinate, often a metal–oxygen distance.

metal transition occurs between the two when the two curves are degenerate. Two possibilities are shown in panels c and d. The normal case, applicable to $La_{1-x}Sr_xMnO_3$ for example, is shown in panel c. The closeness in energy between the copper 3d and oxygen 2p levels means for the cuprates that the "metal" and "insulator" curves of Figure 7d really correspond to the "covalent" and "ionic" curves of the NaCl example noted earlier, a result found by calculation too.[21] The insulating state has holes largely located on copper, the metallic state holes on oxygen. A very crude description of the two might be as $Cu^{2+}O^{2-}$ and $Cu^{+}O^{-}$, respectively. There is then a strong overlap between the two diabatic states.

For the cuprates the interaction between the diabatic curves is large enough to generate a single minimum. The situation is reminiscent of the $Ba_{1-x}K_xBiO_3$ case, described earlier (Figure 4). As shown in Figure 7d such an intersection of the potential energy surfaces may lead to a thermodynamic stabilization at a certain composition. Here the lower adiabatic curve has a minimum which lies deeper than either of the minima associated with the two diabatic curves. We believe that this is the origin of the thermodynamic stabilization at the superconducting composition[20] described in the Introduction. It will only be achieved if the two adiabatic curves are energetically and geometrically similarly located. (They are drawn somewhat separated along $Q = r$(Cu–O) in Figure 7d for clarity.) The strongest interaction will occur when the two curves are degenerate both in energy and in Q.) The resulting 'magic' electronic state is a mixture of the two starting states, ϕ_1 and ϕ_2. The smooth changes in the nature of the electronic state as x increases described by Figure 7a → d → b are reflected in the smooth evolution of properties (e.g., the CuO distance) as the cuprates are doped and the system changes from localized insulator to delocalized metal. The tuning of the two curves to achieve this condition relies on the relative movement of the two curves on doping. Just as in the sodium chloride and $Ba_{1-x}K_xBiO_3$ cases, the charge distributions associated with the two states are different (the localized state containing holes largely on copper and the delocalized state holes largely on oxygen), so that on moving through the interaction region considerable charge transfer occurs (dynamical charge transfer). In contrast to bismuth oxide the composite electronic state is an unusual mixture of (ionic) localized and (covalent) delocalized functions. Thus we would expect that in the region described by the magic electronic state the physical properties should be somewhat unusual.

The Cuprates in More Detail

For both the cuprates and $Ba_{1-x}K_xBiO_3$ during a vibration amplitude the system moves from one electronic description to another. However, the vibrational amplitude is less in $Ba_{1-x}K_xBiO_3$ than the region of r(Bi–O) space over which the adiabatic ground state wave function changes completely, corresponding to the case of Figure 6a. The Bi–O distances corresponding to Bi^{3+}–O and Bi^{5+}–O are quite different. In BCS language the coupling between the two states remains roughly constant during the vibration as indicated by the constant potential V used to derive T_c. For the cuprates the interaction of the two diabatic

(21) Hybertsen, M. S.; Stechel, E. B.; Schluter, M.; Jennison, D. R. *Phys. Rev.* **1990**, *B41*, 11068. Wang, Y. J.; Newton, M. D.; Davenport, J. W. *Phys. Rev.* **1992**, *B46*, 11935. Martin, R. L. In *Cluster Models for Surface and Bulk Phenomena*; Pacchioni, G., Bagus, P. S., Eds.; Plenum: New York, 1992.

curves may be over a much smaller region of configuration space. Our only evidence for this, however, is an inverse argument, that the width of the plots of Figure 2 is less than a typical amplitude of vibration. Thus the interaction between the two curves of Figure 7d, relative to a typical vibration amplitude, may be of the form of **1**. On moving from Figure 7a to 7d and

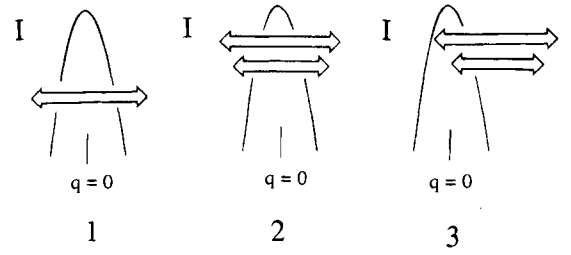

then to 7b the variation in electron–phonon coupling from this source goes through a maximum at the magic electronic state in the same way as T_c of Figure 1. A similar plot holds for the parameter Δc_1^2, the change in the character of the wave function over the amplitude of vibration. This we have suggested is a measure of T_c, although the electronic situation in the cuprates is very different from that in $Ba_{1-x}K_xBiO_3$ where this relationship was derived. The variation in Δc_1^2 as the equilibrium value of q changes by application of pressure or the demands of the reservoir material is shown in Figure 6IV. The plots of Figure 2 have the same shape. The width of the plot will be of the order of magnitude of the vibrational amplitude, and a simple calculation leads to a half-width of around 0.1 Å for a Cu–O stretching vibration located at 600 cm^{-1}. Note that since the Cu–O distance varies with doping level, the T_c/x plot of Figure 1 will be much wider and will not be a good measure of the "homogeneous" width of the process. The electron–phonon coupling appears to take place over a very small part of r(Cu–O) configuration space. That all or the majority of the possible coupling is captured during this vibration leads to the possibility that here is the reason for such high critical superconducting temperatures.

Thus the behavior of a given system depends on the location in configuration space of the minima in the diabatic curves with respect to each other. Clearly, if they are considerably separated, then the electronic situation has to be like that of Figure 6a, where the change in electronic character in the lower adiabatic state takes place over a long distance. Given the difference in bond lengths associated with Bi^{3+} and Bi^{5+} (about 0.10 Å), this is probably of class a. How the interaction between "ionic" and "covalent" curves varies with geometry requires good calculations, and thus the effect of the details of the structure on coupling is beyond us at present. We note, however, that many of the highest T_c systems have flat or nearly flat CuO_2 sheets.

(22) Burdett, J. K. *New J. Chem.* **1993**, *17*, 107.
(23) Bornemann, H. J.; Morris, D. E.; Liu, H. B. *Physica* **1991**, *C182*, 132.

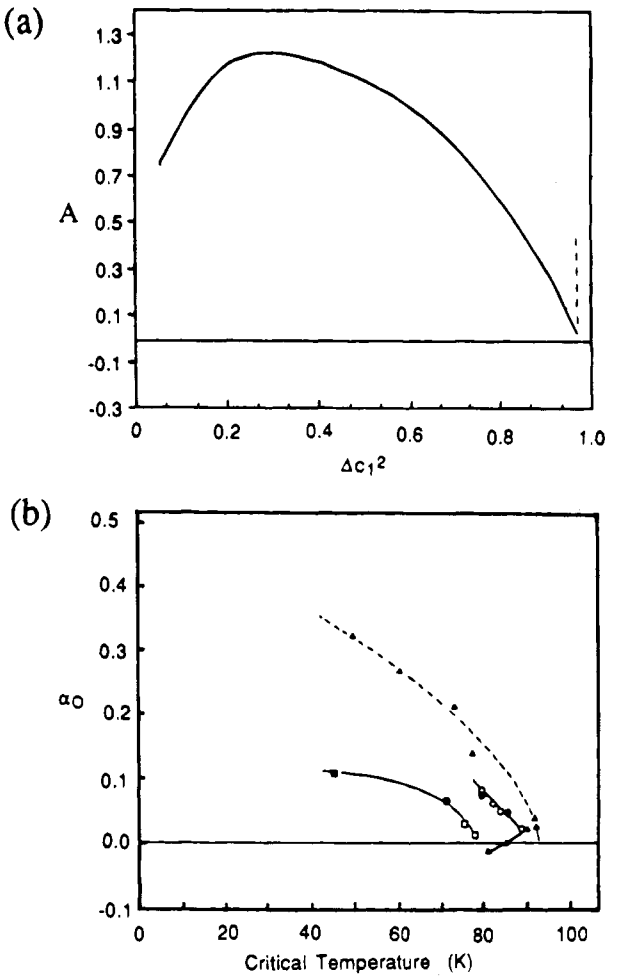

Figure 8. (a) Calculated isotope effect using the model of **2** and **3**. (b) Experimental results from ref 22.

Finally the model can make some comments[22] concerning the isotope effect on T_c, a major prediction of the BCS scheme. If all of the Δc_1^2 is captured (i.e., all of the interaction sampled) during a vibration since the plot of Figure 6cIV is so sharp, then there will be no isotope effect at all. **2** depicts such a situation, showing the amplitudes of two vibrations (the smaller one corresponding to the heavier isotope) superimposed on the interaction I, at $q = 0$. **3** shows amplitudes of two vibrations located away from $q = 0$. Now it is clear that there is an isotope effect. Since from BCS for two isotopes $T_c/T_c' = (\mu'/\mu)^{1/2}$, i.e., $\log(T_c/T_c') = {}^1/_2$, a useful plot to compare with experiment is $\log[(\Delta c_1^2)/(\Delta c_1^2)'] (=A)$ with (Δc_1^2). The theoretical plot of Figure 8a and its comparison with the experimental one of Figure 8b is striking. The correlation with experiment indicates an electron–phonon coupling process which occurs within the width of the vibrational amplitude.

Our research in high-temperature superconductors has been supported by the National Science Foundation (DMR91-20000) through the Science and Technology Center for Superconductivity.

AR940078I